J. Fluid Mech. (1979), *vol.* 94, *part* 4, *pp.* 711–727
Printed in Great Britain

Coriolis-force attenuation of blocking in a stratified flow

By M. R. FOSTER

Department of Aeronautical and Astronautical Engineering,
The Ohio State University, Columbus

(Received 20 September 1976 and in revised form 16 February 1979)

Even very small Coriolis forces are shown to alter significantly the nature of the upstream wake of an object in slow (small Froude number) translation through a non-diffusive stratified fluid. If the Ekman number is of order one, the far upstream extent of the wake is reduced. If the fluid rotation is sufficient to make the Ekman number small, the contraction of the wake is much greater. We study a particular case in detail; the Ekman number is small enough to make horizontal boundary layers Ekman layers. In this case, the wake is confined to the vicinity of the object, the upstream flow arising from a combination of Ekman pumping and baroclinic vorticity generation. The upstream flow is described by an eigenfunction whose amplitude is dependent on object geometry. If the object is a semi-infinite rectangular parallelepiped, that amplitude is determined by detailed examination of the shear layer at the face of the parallelepiped and its interaction with the Ekman layer on the top surface of the object.

1. Introduction

When a stably stratified fluid flows slowly past an obstacle, a very long upstream wake forms in which the fluid is nearly stagnant. This 'blocking' phenomenon has been reviewed along with other features of stratified flows by Yih (1969) and more recently by Barnard & Pritchard (1975). This paper deals with the effects of rather weak Coriolis forces on the motion and, in particular, on the upstream wake.

If the density stratification arises from a solute that has a large Schmidt number, such as salt in water, then the fluid may be treated to a first approximation as though the diffusion coefficient were, in fact, zero. This means that there are very thin layers adjoining the solid surfaces in which the necessary density adjustments occur. Such a non-diffusive assumption has been utilized by a number of authors in constructing solutions for flow past a variety of obstacles, e.g. Martin & Long (1968), Graebel (1969), Janowitz (1971), and Foster (1977). We proceed here with the same sort of non-diffusive model.

As we shall see, even exceedingly small Coriolis forces, relative to buoyancy forces, produce considerable changes in the upstream flow. Indeed, we show below that for rotation large enough to make the Ekman number based on fluid-layer depth small, the effect of the Coriolis forces is to remove the blocked, stagnant region that exists upstream of the obstacle in the absence of rotation.

The parameter that measures the dynamical importance of Coriolis forces as compared with the buoyancy forces is

$$R \equiv \frac{\Omega U}{N^2 h},$$

0022–1120/79/4300–7140 $02.00

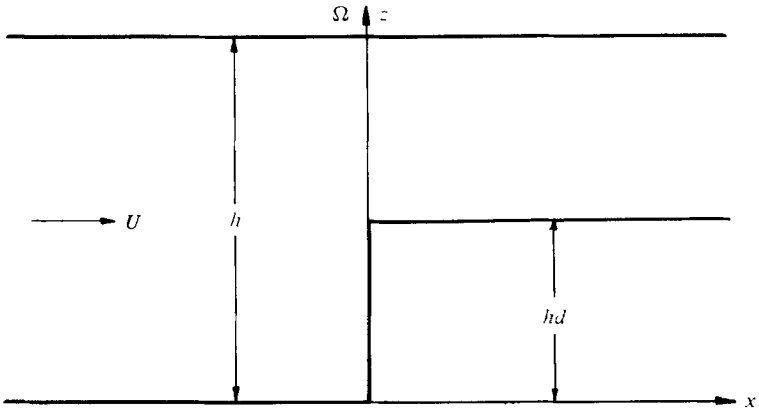

FIGURE 1. Co-ordinate system for flow past a semi-infinite rectangular parallelepiped.

where Ω is the angular velocity of the co-ordinate frame; U is the speed of the obstacle through the fluid; h, the fluid layer depth; and N, the Brunt–Väisälä frequency. This number is the ratio of the square of the Froude number and the Rossby number.

If one compares viscous forces and buoyancy forces, the parameter that results is

$$\epsilon \equiv \frac{\nu U}{N^2 h^3}.$$

Here, ν is the kinematic viscosity of the fluid; ϵ is the product of square of the Froude number and the inverse Reynolds number, ν/Uh. We will assume throughout the analysis that the Froude number, U/Nh, is small. We will also take ϵ to be small, which means that viscous effects will be confined to thin boundary and shear layers.

In § 2, we show that blocking may occur only if $R \ll \epsilon \ll 1$, provided also that the Froude number is small. We then discuss briefly the various flow regimes that arise for different relative orders of R and ϵ. The remainder of the paper deals with the solution for a particular ordering of R and ϵ, viz., when R is of order $\epsilon^{\frac{1}{2}}$, which turns out to be an especially interesting case.

When $R = O(\epsilon^{\frac{1}{2}})$, the Coriolis forces are of sufficient size that the horizontal surface boundary layers are Ekman layers. Upstream of the obstacle, the fluid is pumped vertically upward by the Ekman layers. The upward motion in the gravitational field creates streamwise vorticity which deflects the stream laterally as it approaches the obstacle. This lateral stream deflexion increases the Ekman pumping which increases the vorticity production, thereby increasing the stream deflexion, and so on and on. Such a positive feedback mechanism gives rise to a vertical motion that grows exponentially as the fluid approaches the obstacle from upstream. This process is clearly independent of the details of the shape of the obstacle itself. In fact, the only way in which the obstacle geometry affects the upstream flow is in the magnitude of the flow deflexion. This sort of eigenfunction in the upstream flow is also an essential feature of supersonic laminar boundary-layer separation (see Stewartson 1964, p. 150, for example).

In this paper, we fix attention on a particular obstacle, a semi-infinite prism (see figure 1). We give upstream and downstream solutions for this geometry in § 4. Straddling the step at $x = 0$ is a thin viscous shear layer of width $h(\epsilon/R^2)^{\frac{1}{4}}$. The Ekman

layers, with thickness $(\epsilon/R)^{\frac{1}{2}}h$ in these parameters, are much thinner and flow beneath the thicker shear layer. The shear layer interacts strongly with the Ekman layer beneath it at the 270° corner, internal to the shear layer. The interaction is described in detail in § 5, the numerical solution to the shear layer equations being outlined in § 6. The details of the shear layer structure are important since they determine the amplitude of the upstream eigenfunction in the outer flow.

2. Formulation

We now consider an incompressible fluid, which is stably stratified, that occupies the space between two parallel plates whose normal is aligned with gravity. The plates are separated by a distance h, and the entire container rotates rapidly about the surface normals at angular speed Ω. A two-dimensional object is in motion through the fluid, sliding along the bottom wall, at speed U right-to-left (see figure 1). Though much of what follows is quite general, the particular obstacle to be considered in detail later is a semi-infinite rectangular parallelepiped of height hd. Foster (1977) has given the solution for the motion due to such an obstacle in the absence of rotation. To describe the flow structure in a steady frame, we use co-ordinates fastened to the moving obstacle.

In that reference frame, the equations of motion under a Boussinesq approximation are

$$\nabla.\mathbf{u} = 0, \tag{2.1}$$

$$(\mathbf{u}.\nabla)\mathbf{u} + 2\boldsymbol{\Omega}\times\mathbf{u} + \nabla p = \nu\nabla^2\mathbf{u} - \rho g\mathbf{k}, \tag{2.2}$$

$$\mathbf{u}.\nabla\rho = 0, \tag{2.3}$$

where $\mathbf{u}$ is the fluid velocity vector, p is the reduced pressure divided by the mean density, and ρ is the ratio of the density to the mean density; g is the acceleration of gravity and $\boldsymbol{\Omega}$ is aligned with $\mathbf{k}$, the z unit vector. The boundary conditions in this co-ordinate system are

$$\mathbf{u} = U\mathbf{i} \quad \text{on} \quad \begin{cases} z = h \\ z = 0, \quad x < 0 \quad \text{and} \quad x > L, \end{cases} \tag{2.4}$$

if the object has horizontal extent L on $x = 0$. In this reference frame the object is at rest, so

$$\mathbf{u} = 0 \quad \text{on the object.} \tag{2.5}$$

Far upstream, the fluid is undisturbed, so

$$\left.\begin{array}{l} \rho \sim 1 - \beta z, \quad \beta > 0, \\ \mathbf{u} \sim U\mathbf{i}. \end{array}\right\} \quad x \to -\infty. \tag{2.6}$$

Equation (2.3) has the general solution

$$\rho = \rho(\psi), \tag{2.7}$$

where ψ is the stream function,

$$u = \frac{\partial\psi}{\partial z}, \quad w = -\frac{\partial\psi}{\partial x}. \tag{2.8}$$

In that region of the flow covered by streamlines originating at $x = -\infty$, (2.7) and (2.6) indicate that

$$\rho = 1 - (\beta/U)\psi. \tag{2.9}$$

Introducing (2.9) into (2.2) eliminates ρ as a dependent variable and the result is

$$(\mathbf{u}.\nabla)\mathbf{u} + 2\boldsymbol{\Omega} \times \mathbf{u} + \nabla p_1 = \nu\nabla^2\mathbf{u} + (g\beta/U)\psi\mathbf{k}, \tag{2.10}$$

where p_1 is $p + gz$. A steady velocity $U\mathbf{i}$ upstream causes a Coriolis force which must be balanced by pressure gradient in the y direction. Thus, we write

$$p = -gz - 2\Omega U y + g\beta h^2 p^*,$$

$$\mathbf{u} = U\mathbf{u}^*, \quad \psi = Uh\psi^*, \quad \mathbf{x} = h\mathbf{x}^*,$$

and substitute into (2.1) and (2.10) to obtain a set of dimensionless equations in * quantities. Dropping the *, those equations are

$$\nabla.\mathbf{u} = 0, \tag{2.11}$$

$$F^2(\mathbf{u}.\nabla)\mathbf{u} + 2FS\mathbf{k} \times (\mathbf{u} - \mathbf{i}) + \nabla p = \epsilon\nabla^2\mathbf{u} + \psi\mathbf{k}. \tag{2.12}$$

The parameters characterizing the solution are

$$F \equiv \frac{U}{(g\beta h^2)^{\frac{1}{2}}}, \quad S \equiv \frac{\Omega}{(g\beta)^{\frac{1}{2}}}, \quad \epsilon \equiv \frac{\nu U}{g\beta h^3} = F^2/Re.$$

F is a modified Froude number which we shall hereafter suppose to be sufficiently small to allow neglect of the nonlinear term in (2.12). S is a measure of the relative importance of buoyancy and Coriolis forces, and ϵ, a measure of viscous forces. Neglect of the inertia of the fluid in favour of viscous forces apparently means from (2.12) that F must be small compared to $\epsilon^{\frac{1}{2}}$, or simply small Reynolds number. A proper restriction on F arises later and will be discussed in § 7. We deal also in § 7 with the nature of the restriction on the Schmidt number, not shown here.

In the absence of fluid inertia, F and S occur in (2.12) as a product only, so we define $R = FS$. The slow flow equations ($F \ll \epsilon^{\frac{1}{2}}$) are then

$$\nabla.\mathbf{u} = 0, \tag{2.13}$$

$$2R\mathbf{k} \times (\mathbf{u} - \mathbf{i}) + \nabla p = \epsilon\nabla^2\mathbf{u} + \psi\mathbf{k}. \tag{2.14}$$

The non-dimensional version of the boundary conditions (2.4), (2.5) is

$$\mathbf{u} = \mathbf{i} \quad \text{on} \quad \begin{cases} z = 1 \\ z = 0, \quad x < 0 \quad \text{and} \quad x > L/h, \end{cases}$$

$$\mathbf{u} = \mathbf{0} \quad \text{on the object,} \tag{2.15}$$

and the upstream condition is

$$\mathbf{u} \sim \mathbf{i}, \quad x \to -\infty. \tag{2.16}$$

Range of R	x extent of upstream wake	Solution
$\epsilon^{\frac{1}{2}} \ll R$	$O(1)$, if at all	$u = 1$
$\epsilon \ll R \ll \epsilon^{\frac{1}{2}}$	$O(\epsilon/R^2)$	(3.2)
$R \ll \epsilon$	$O(1/\epsilon)$	(3.4)

TABLE 1

3. The far-upstream structure

Since $|z| < 1$ in the region occupied by the fluid, for x large, rates of change with respect to x will become very small compared to z rates of change. Under such an approximation, elimination of p in (2.14) and use of (2.13) gives

$$\epsilon \frac{\partial^4 u}{\partial z^4} - \frac{\partial u}{\partial x} + \frac{4R^2}{\epsilon}(u-1) = 0. \tag{3.1}$$

Graebel (1969) obtained this equation with $R \equiv 0$ by similar reasoning. For $R \gg \epsilon^{\frac{1}{2}}$, the final term is dominant so $u \equiv 1$ far upstream and any influence of the obstacle, if such exists, is felt near [meaning $x = O(1)$] the obstacle only. This is the case for strong rotation. However, for $\epsilon \ll R \ll \epsilon^{\frac{1}{2}}$, when the rotation is a bit weaker, the final two terms balance and

$$u \sim 1 + C(z) \exp(4R^2 x/\epsilon), \quad x \to -\infty. \tag{3.2}$$

The function $C(z)$ clearly depends upon the exact nature of the flow disturbance near $x = 0$.

For $R \ll \epsilon$, the first two terms are in balance,

$$\frac{\partial^4 u}{\partial z^4} - \frac{\partial u}{\partial(\epsilon x)} = 0. \tag{3.3}$$

It may be easly shown, with reference to Foster (1977), that the asymptotic solution of (3.3) is

$$u \sim 1 + A_1 \phi_1(z) \exp(k_1^4 \epsilon x), \quad x \to -\infty, \tag{3.4a}$$

where k_1 is an eigenvalue, 4·73004, and ϕ_1 an eigenfunction given by

$$\phi_1(z) = \sin(k_1 z) + \sinh(k_1 z) + (\cot k_1 - \operatorname{cosec} k_1)(\cos(k_1 z)) - \cosh(k_1 z)). \tag{3.4b}$$

In terms of far-upstream flow disturbance, we summarize the results in table 1. The entry $R \ll \epsilon$ is equivalent to large Ekman number, $\nu/\Omega h^2$. If $R = O(\epsilon)$, then the solution is of the complete equation (3.1) which may be easily shown to be (3.4a) with A_1 multiplied by the factor $\exp(4R^2 x/\epsilon)$.

In conclusion, there is far-upstream penetration of the wake only for

$$S = O(Re^{-\frac{1}{2}}). \tag{3.5}$$

4. The solution for $R = O(\epsilon^{\frac{1}{3}})$; the outer flow

We now construct the solution to (2.13), (2.14) for $R \ll 1$, with $R = O(\epsilon^{\frac{1}{3}})$; the boundary conditions are given by (2.15). We proceed by putting $\epsilon = \sigma R^3$, where σ is of order unity. Equations (2.13) and (2.14) then become

$$\nabla . \mathbf{u} = 0, \tag{4.1}$$

$$2R\mathbf{k} \times (\mathbf{u} - \mathbf{i}) + \nabla p = \sigma R^3 \nabla^2 \mathbf{u} + \psi \mathbf{k}. \tag{4.2}$$

The outer expansion for $R \to 0$ is

$$\begin{aligned} \begin{pmatrix} u \\ w \end{pmatrix} &= \begin{pmatrix} u_0 \\ w_0 \end{pmatrix} + R \begin{pmatrix} u_1 \\ w_1 \end{pmatrix} + \ldots, \\ v &= R^{-1} v_0 + v_1 + \ldots, \\ p &= p_0 + R p_1 + \ldots, \end{aligned} \tag{4.3}$$

and substitution into (4.1), (4.2) yields, on elimination of p_0,

$$u_0 = 1, \tag{4.4a}$$

$$2\frac{\partial v_0}{\partial z} + w_0 = 0, \tag{4.4b}$$

$$\frac{\partial w_0}{\partial z} = 0. \tag{4.4c}$$

For $\sigma = O(1)$, Ekman layers exist on all non-vertical surfaces in the flow, so the Ekman compatibility conditions may be appended to (4.4) to account for the presence of the boundaries.

The upstream solution

In $x < 0$, the boundaries are $z = 0$ and $z = 1$, and the Ekman conditions are

$$w_0 = \pm \tfrac{1}{2}\sigma^{\frac{1}{2}} \frac{\partial v_0}{\partial x} \quad \text{on} \quad z = \begin{cases} 0 \\ 1 \end{cases}. \tag{4.5}$$

Since (4.4*c*) indicates $w_0 = w_0(x)$, (4.4*b*) may be integrated to give

$$v_0 = A(x) - w_0 z/2, \tag{4.6}$$

and $A(x)$ is as yet an arbitrary function. Application of the conditions (4.5) to the solution (4.6) results in an equation for A in terms of w_0 and

$$\frac{dw_0}{dx} - \frac{8}{\sigma^{\frac{1}{2}}} w_0 = 0. \tag{4.7}$$

The solution is

$$w_0 = C \exp(8x/\sigma^{\frac{1}{2}}), \tag{4.8}$$

and v_0, from (4.6), is

$$v_0 = \tfrac{1}{2}C(\tfrac{1}{2} - z) \exp(8x/\sigma^{\frac{1}{2}}). \tag{4.9}$$

We note that the structure of the upstream flow given by (4.8) and (4.9) is independent of the details of the disturbance in the channel. Only the value of the constant C is dependent on the character of the flow disturbance.

The downstream solution

The results (4.8), (4.9) are quite general. However, the downstream ($x > 0$) structure is strongly obstacle-dependent, and so we suppose for definiteness that the object is, as indicated in § 2, a semi-infinite rectangular parallelepiped whose top face is at $z = d$ in $x > 0$. The equations (4.4) are obviously still applicable downstream. Note that, from (4.4*a*), the volume flux in the fluid over the prism is $(1-d)$, whereas a flux of unity *must* be carried downstream. The Ekman layers on $z = d$ and $z = 1$ each carry, to leading order, a flux of amount (see Greenspan 1964, p. 46)

$$-\tfrac{1}{2}\sigma^{\frac{1}{2}}v_0,$$

so, if the excess flux d is to be carried by the Ekman layers, clearly v_0 must be given by

$$v_0 = -d/\sigma^{\frac{1}{2}}. \tag{4.10}$$

Actually, if the object is *not* a rectangular parallelepiped, but another semi-infinite solid with a vertical face of height d at $x = 0$, it is easy to show that (4.10) should be replaced by

$$v_0 = \frac{-2d/\sigma^{\frac{1}{2}}}{1+(1+(f')^2)^{\frac{1}{2}}}, \tag{4.11}$$

where $f'(x)$ is the slope of the top of such an obstacle. Bearing in mind that this generalization is easily made (for all shapes for which $f'(0) < \infty$), we deal below with (4.10).

We now summarize the first-order outer solution for flow caused by the motion of the rectangular parallelepiped, namely

$$\left.\begin{aligned} u_0 &= 1, \\ v_0 &= \begin{cases} \tfrac{1}{2}C(\tfrac{1}{2}-z)\exp(8x/\sigma^{\frac{1}{2}}), & x < 0, \\ -d/\sigma^{\frac{1}{2}}, & x > 0, \end{cases} \\ w_0 &= \begin{cases} C\exp(8x/\sigma^{\frac{1}{2}}), & x < 0, \\ 0, & x > 0, \end{cases} \end{aligned}\right\} \tag{4.12}$$

The constant C is not yet determined, and may only be determined by the careful investigation of the structure of the vertical shear layer on $x = 0$, which we undertake in § 5.

5. The vertical shear layer

At $x = 0$, there exists a thin vertical shear layer which smooths the discontinuities of v_0 and w_0 indicated in (4.12). The usual thin-layer approximations applied to (2.13), (2.14) give

$$\frac{\partial u}{\partial x}+\frac{\partial w}{\partial z} = 0, \tag{5.1}$$

$$\sigma R^3\frac{\partial^3 w}{\partial x^3}-w = 2R\frac{\partial v}{\partial z}, \tag{5.2}$$

$$\sigma R^2\frac{\partial^3 v}{\partial x^3} = -2\frac{\partial w}{\partial z}. \tag{5.3}$$

Equations (5.2), (5.3) would be the familiar Stewartson layer equations were it not for the '$-w$' term in (5.2), arising from fluid buoyancy. A careful study of the equations shows that there are two distinct layers. The thinner layer has width $\sigma^{\frac{1}{3}}R$ and does not arise in this context.

The thicker layer has width $(\sigma R)^{\frac{1}{4}}$. Writing $x = (\sigma R)^{\frac{1}{4}}\xi$ and substituting into (5.2) and (5.3) gives

$$\frac{\partial^3 v}{\partial \xi^3} = 4\frac{\partial^2 v}{\partial z^2}, \tag{5.4}$$

$$2R\frac{\partial v}{\partial z} + w = 0, \tag{5.5}$$

$$2(u-1) = \sigma^{\frac{1}{2}}R^{\frac{1}{2}}\frac{\partial^2 v}{\partial \xi^2}, \tag{5.6}$$

where terms of order $R^{\frac{1}{2}}$ have been neglected. The Ekman layer is of width R, and so penetrates underneath this relatively thicker layer. The Ekman compatibility condition in these variables is, from (4.5),

$$w = \pm\tfrac{1}{2}\sigma^{\frac{1}{8}}R^{\frac{3}{8}}\frac{\partial v}{\partial \xi} \quad \text{on} \quad z = \begin{cases} 0, & \xi < 0; \quad d, \xi > 0, \\ 1. \end{cases} \tag{5.7}$$

The sizes of v and w in this shear layer are determined by matching to the outer solution, (4.12). Writing $x = (\sigma R)^{\frac{1}{4}}\xi$ in (4.12) and expanding for $(\sigma R)^{\frac{1}{4}} \to 0$, we obtain the matching conditions for the layer solutions, namely,

$$u \sim 1, \quad |\xi| \to \infty, \tag{5.8}$$

$$\left.\begin{aligned} v &\sim \begin{cases} \tfrac{1}{2}CR^{-1}(\tfrac{1}{2}-z) + O(R^{-\frac{3}{8}}\xi), & \xi \to -\infty, \\ -dR^{-1}\sigma^{\frac{1}{4}}, & \xi \to +\infty, \end{cases} \\ w &\sim \begin{cases} C + O(R^{\frac{1}{8}}\xi), & \xi \to -\infty, \\ 0, & \xi \to +\infty. \end{cases} \end{aligned}\right\} \tag{5.9}$$

In addition to matching to the outer flow as indicated by (5.9), solutions to (5.4)–(5.6) must also obey the no-slip condition on $\xi = 0$, $0 < z < d$. Equation (5.5) indicates that, if $v = 0$ there, then $w = 0$ also. For u to be zero, (5.6) indicates $\partial^2 v/\partial \xi^2$ must have a particular value, so the boundary conditions are

$$\left.\begin{aligned} v &= 0 \\ \frac{\partial^2 v}{\partial \xi^2} &= -\frac{2}{\sigma^{\frac{1}{2}}R^{\frac{1}{2}}} \end{aligned}\right\} \quad \text{on} \quad \xi = 0, \quad 0 \leqslant z \leqslant d. \tag{5.10}$$

Examination of (5.9) and (5.10) indicates that the shear layer solution should have the following expansion:

$$\left.\begin{aligned} v &= \sigma^{-\frac{1}{3}}R^{-\frac{1}{3}}V_0 + R^{-1}V_1 + \ldots, \\ w &= \sigma^{-\frac{1}{3}}R^{-\frac{1}{3}}W_0 + W_1 + \ldots, \end{aligned}\right\} \tag{5.11}$$

where upper case letters hereafter denote shear layer solutions.

The *leading-order* equations from substitution into (5.4) and (5.5) are

$$\frac{\partial^3 V_0}{\partial \xi^3} = 4\frac{\partial^2 V_0}{\partial z^2},$$

$$W_0 = -2\frac{\partial V_0}{\partial z}, \tag{5.12}$$

and the boundary condition is

$$V_0 = 0 \tag{5.13a}$$

$$\frac{\partial^2 V_0}{\partial \xi^2} = -2 \quad \text{on} \quad \xi = 0, \quad 0 \leqslant z \leqslant d. \tag{5.13b}$$

The matching conditions indicate that

$$V_0, W_0 \to 0, \quad |\xi| \to \infty. \tag{5.14}$$

Substitution of (5.11) into the Ekman condition, (5.8), indicates that $\partial V_0/\partial \xi$ must vanish on horizontal boundaries. That together with (5.14) yields

$$V_0 = 0 \quad \text{on} \quad z = 1; \quad z = 0, \quad \xi < 0; \quad z = d, \quad \xi > 0. \tag{5.15}$$

Discussion of the shear-layer solution

Because of the complexity of the analysis to follow, it is appropriate to first discuss the physical mechanism inherent in the solution. Since the boundary condition on the horizontal surfaces is, from (5.15), $V = 0$, it is clear from (5.12) that W will not in general be zero on those surfaces. This means that fluid in the shear layer flows in and out of the much thinner Ekman layers on these horizontal surfaces. The volume flux associated with the V_0 solution is order unity, the same as the order of the volume flux in the Ekman layers in the outer flow upstream and downstream of the shear layer.

Therefore, the shear layer rearranges the volume of fluid flowing in the Ekman layers beneath and above it. In particular, the net volume flux entering the Ekman layer under the shear layer on $z = d$, from $\xi = 0$ to $\xi = \infty$ *must* be $\frac{1}{2}d$,† the volume flux carried by the Ekman layer on $z = d$ in the flow downstream of the layer. So we require

$$\int_0^\infty W_0\Big|_{z=d} d\xi = -\tfrac{1}{2}d. \tag{5.16}$$

Since (5.12)–(5.15) constitute a well-posed parabolic problem, one *cannot* append an additional condition (5.16). We show, however, that (5.13) must be slightly modified to allow for a singularity in the solution at the 270° corner at $\xi = 0, z = d$. Proper choice of this singularity strength makes satisfaction of (5.16) possible. The singularity owes its existence to shear layer–Ekman layer interaction, a feature noted in a somewhat similar situation by Moore & Saffman (1969). As in their case, a family of singularities exists, and we choose the weakest singularity.

† This assumes there is no source-like Ekman layer eruption at $\xi = 0$. That is confirmed by the appendix.

The structure of the solution

As indicated above, solution of (5.12)–(5.15) cannot also satisfy (5.16). We now, in anticipation of possible shear layer–Ekman layer interaction, resulting in singularities at $z = 0$, $\xi = 0-$ or $z = d$, $\xi = 0+$, replace (5.13) by

$$\left.\begin{aligned} V_0 &= 0 \\ \frac{\partial^2 V_0}{\partial \xi^2} &= -2 + 2f(z) \end{aligned}\right\} \quad \text{on} \quad \xi = 0, \quad 0 \leqslant z \leqslant d, \tag{5.17}$$

where $f \equiv 0$ except near $z = 0$ and/or $z = d$.

Integrating (5.12a) over the portion of the shear layer in $z \geqslant d$, we obtain, also by using (5.14),

$$\int_{-\infty}^{\infty} V_0 \, d\xi = A(1-z). \tag{5.18}$$

A is a constant to be determined. Integration of the same equation in $0 \leqslant z \leqslant d$, $-\infty < \xi \leqslant 0$, using (5.17), leads to

$$\int_{-\infty}^{0} V_0 \, d\xi = -\tfrac{1}{4}z^2 + Bz + \tfrac{1}{2}\int_0^z (z-s) f(s) \, ds, \tag{5.19}$$

where B is another integration constant.

A and B are not independent since V_0 is continuous on $z = d$, $\xi < 0$ and zero on $z = d$, $\xi > 0$. Thus,

$$B = \tfrac{1}{4}d + \frac{A(1-d)}{d} - \frac{1}{2d}\int_0^d (d-s) f(s) \, ds. \tag{5.20}$$

Using (5.12b), we can write

$$\int_{-\infty}^{\infty} W_0 \, d\xi = 2A,$$

and

$$\int_{-\infty}^{0} W_0 \, d\xi = z - \tfrac{1}{2}d - \frac{2A(1-d)}{d} + \int_z^d f(s) \, ds - \frac{1}{d}\int_0^d s f(s) \, ds. \tag{5.21}$$

Evaluating both of these expressions at $z = d$, we subtract (5.21b) from (5.21a). Continuity of W_0 on $z = d$, $\xi < 0$, then leads to

$$\int_0^{\infty} W_0\Big|_{z=d} \, d\xi = -\tfrac{1}{2}d + \frac{2A}{d} + \frac{1}{d}\int_0^d s f(s) \, ds. \tag{5.22}$$

Comparing with (5.16), we see that f must be such that

$$\int_0^d s f(s) \, ds = -2A. \tag{5.23}$$

Whatever singularities are inherent in f, their strength must be such as to satisfy (5.23). Recall also that (5.21a) may be written as

$$A = -\int_{-\infty}^{\infty} \frac{\partial V_0}{\partial z}\Big|_{z=1} \, d\xi. \tag{5.24}$$

In the appendix, singular solutions to (5.12) near 90° and 270° corners are found in a

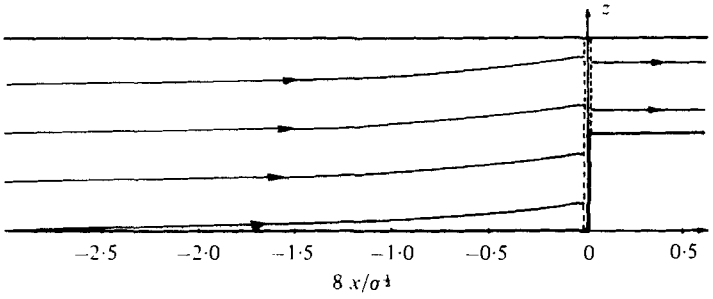

FIGURE 2. Outer flow streamlines for a semi-infinite rectangular parallelepiped with $d = \frac{1}{2}$. The shear layer location is shown schematically by the broken lines.

fashion very like that employed by Moore & Saffman (1969). A number of eigenfunctions are determined in each case. We show there that, though there are no source-like solutions at either corner, a doublet-like singularity may occur at the 270° corner. Now, since the singularity occurs over a region that is $o(1)$ in z, it is equivalent, so far as the shear layer solution is concerned, to the generalized function $\delta'(z-d)$. Satisfaction of (5.23) determines its amplitude, hence

$$f(z) = 2A\delta'(z-d-). \tag{5.25}$$

Therefore, the shear layer problem is constituted by (5.12), (5.14), (5.15) and, replacing (5.13),

$$\partial^2 V_0/\partial\xi^2 = -2+4A\delta'(z-d-) \text{ on } \quad \xi = 0, \quad 0 \leqslant z \leqslant d. \tag{5.26}$$

Connexion of A and C

The inviscid solution of § 3 indicates that the volume flux in the Ekman layer on $z = 1-$ in $x < 0$, as it enters the shear layer from the left, is

$$\frac{\sigma^{\frac{1}{2}}}{8}C,$$

and also that the volume flux in that same Ekman layer leaving the shear layer on the right is $\frac{1}{2}d$. The difference in these, $\sigma^{\frac{1}{2}}C/8-\frac{1}{2}d$, must be the net downward flux inside the shear layer at $z = 1$, $-2A$. Therefore

$$C = \frac{4}{\sigma^{\frac{1}{2}}}(d-4A). \tag{5.27}$$

So the solution in the outer flow is dependent on the shear layer structure through the value of A. In § 6 we discuss the numerical means of obtaining values for A. We find there that, for $d = \frac{1}{2}$, $A = 0{\cdot}0566$ and therefore $\sigma^{\frac{1}{2}}C/4 = 0{\cdot}274$. Figure 2 shows the streamlines for $d = \frac{1}{2}$ using this value of C in (4.8).

6. Numerical solution of the shear layer equation

In this section, we describe the method of obtaining a solution to (5.12) subject to conditions formulated in § 5,

$$V = 0 \quad \text{on} \quad z = 1; \quad z = 0, \quad \xi < 0; \quad z = d, \quad \xi > 0; \quad \xi = 0, \quad z < d; \tag{6.1}$$

$$\partial^2 V/\partial \xi^2 = -2 + 4A\delta'(z - d-), \quad \xi = 0, \quad z \leqslant d; \tag{6.2}$$

and

$$\int_{-\infty}^{\infty} \left.\frac{\partial V}{\partial z}\right|_{z=1} d\xi = -A. \tag{6.3}$$

We proceed by writing

$$V = \left(1 - \frac{\pi^2 A}{d^2}\right) V^{(1)} - \frac{\pi^2}{d^2} A V^{(2)} - A \frac{\partial^2 V^{(2)}}{\partial z^2}, \tag{6.4}$$

where $V^{(1)}$ and $V^{(2)}$ are each solutions of (5.12), subject to (6.1). It is important to note that if $V^{(2)}$ is a solution to (5.12) satisfying (6.1), then $\partial^2 V^{(2)}/\partial z^2$ is *also* a solution. Therefore, (6.4) represents V as a linear combination of three solutions. The particular form of (6.4) follows from the conditions on $\xi = 0$, $z < d$, namely

$$\frac{\partial^2 V^{(1)}}{\partial \xi^2} = -2, \tag{6.5a}$$

$$\frac{\partial^2 V^{(2)}}{\partial \xi^2} = 2(1 - \cos(z\pi/d)), \quad \text{on} \quad \xi = 0, \quad z < d. \tag{6.5b}$$

Careful differentiation of (6.4) and substitution into (6.2) shows that indeed that condition *is* satisfied. Having obtained $V^{(1)}$ and $V^{(2)}$ for (6.4), one can calculate

$$Q^{(l)} \equiv \int_{-\infty}^{\infty} \left.\frac{\partial V^{(l)}}{\partial z}\right|_{z=1} d\xi, \quad l = 1, 2. \tag{6.6}$$

Notice that since $\partial^2 V^{(2)}/\partial z^2$ is proportional to the third ξ derivative of $V^{(2)}$, by (5.12), the Q associated with that solution is easily seen to be exactly zero. Differentiation of (6.4) by z then yields

$$A = \frac{-Q^{(1)}}{1 - (\pi^2/d^2)(Q^{(1)} + Q^{(2)})}. \tag{6.7}$$

Thus, the parameter A of the solution is evaluated and can be used in (6.4) to determine V completely.

The numerical method

The rationale for choosing $V^{(1)}$ and $V^{(2)}$ in the way described is that the boundary data is smooth, thus eliminating the difficult handling of δ' in a numerical procedure. Numerically, then, we have to solve (5.12) with conditions (6.1) and (6.5), so we write (6.5) generically as

$$\frac{\partial^2 V}{\partial \xi^2} = F(z) \quad \text{on} \quad \xi = 0, \quad z < d.$$

We proceed by writing (5.12) in finite difference form in the usual fashion, using differences centred both in ξ and z. The result is

$$-\lambda v_{i-2,j} + 2\lambda v_{i-1,j} + v_{i,j} - 2\lambda v_{i+1,j} + \lambda v_{i+2,j} = \tfrac{1}{2}(v_{i,j-1} + v_{i,j+1}), \tag{6.8}$$

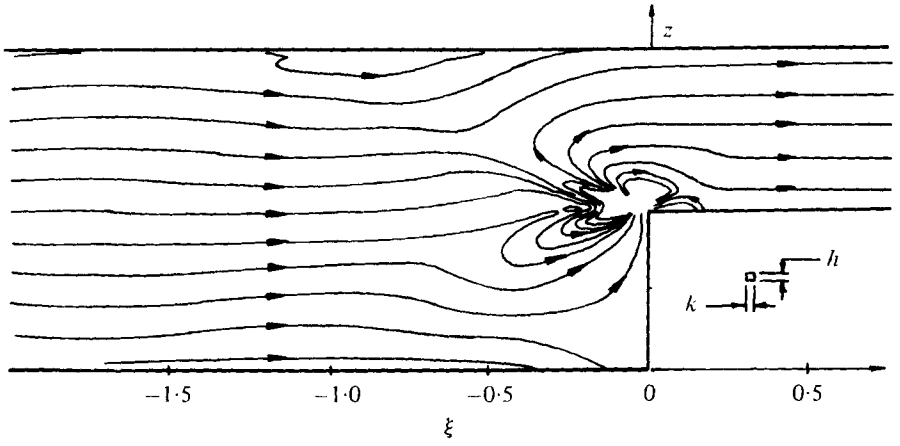

FIGURE 3. Shear layer streamlines for $d = \frac{1}{2}$. The plot is for the case $k = h = 0{\cdot}02$, so fine resolution near the corner is not possible. The mesh size is shown in the figure for comparison. The stream function differs by 0·1 on adjacent lines.

where $\lambda \equiv h^2/16k^3$; h is the z spacing in the grid and k is the ξ step size. The errors in this differencing are $O(h^2)$ and $O(k^2)$. The first subscript refers to the ξ direction, and the second to the z direction. The boundary conditions are easily written down, and (6.8) is solved by relaxation. We use a line-relaxation method, sweeping the grid from $z = 0$ to $z = 1$; such a procedure involves inversion of a penta-diagonal matrix on each line, which can be done very efficiently (using DGELB in the IBM SSP library), and this method converges much faster than point-relaxation (O. R. Burggraf 1977, private communication).

Since the ξ range is doubly infinite, at the ξ boundaries of the grid we require that v have the proper asymptotic structure. It is easy to verify from (5.12) that

$$\begin{aligned} V &\sim (A\exp[\beta\xi] + \bar{A}\exp[\bar{\beta}\xi])\sin(\pi z), \quad \xi \to -\infty, \\ V &\sim Be^{-\gamma\xi}\sin\left(\frac{\pi(z-d)}{1-d}\right), \quad \xi \to +\infty, \end{aligned} \tag{6.9}$$

where

$$\beta = (2\pi)^{\frac{1}{3}}\exp[i\pi/3], \quad \gamma = \left(\frac{2\pi}{1-d}\right)^{\frac{1}{3}},$$

and $\bar{\ }$ denotes complex conjugate.

All calculations were done in double precision (64 bit) arithmetic on the IBM 370 of the Ohio State University Instruction and Research Computer Center. Truncation error studies were performed, with the most accurate solution obtained characterized by h and k of 0·01 in a grid 100 by 500. Throughout the calculations, iteration termination occurred with repeatability errors of less than 0·0001.

Computed values of $Q^{(1)}$ and $Q^{(2)}$ had to be adjusted to account for the exponential tails of the solutions not included because of the finite size of the ξ domain. Equation (6.9) supplies an analytical Q correction. We used h^2 extrapolation to obtain accurate values of $Q^{(1)}$ and $Q^{(2)}$. For $d = \frac{1}{2}$, those are

$$\begin{aligned} Q^{(1)} &= -0{\cdot}0285, \\ Q^{(2)} &= 0{\cdot}0411. \end{aligned} \tag{6.10}$$

Using (6.7), we compute A to be 0·0566. Shear layer streamlines were obtained and are shown in figure 3.

7. Final remarks

The solution presented in §§ 3–6 was predicated on two assumptions, namely that both the diffusivity of the fluid and its inertia may be neglected. As stated in § 2, neglect of the fluid inertia in general requires that $F \ll \epsilon^{\frac{1}{2}}$. In terms of the analysis of §§ 3–6, that means $F \ll R^{\frac{3}{2}}$. This requirement can be lessened somewhat by looking in detail at the shear-layer and Ekman-layer equations. The more severe restriction on the order of F comes from the requirement that radial transport of angular momentum be negligible in the shear layer,

$$F \ll R^{\frac{4}{3}} \sigma^{\frac{1}{3}}. \tag{7.1}$$

For the effects of diffusion to be negligible in the inviscid flow upstream and downstream of the prism face, it is necessary that the Péclet number, Uh/κ, be large compared with unity. However, the effects of non-zero diffusivity will modify the Ekman layers unless

$$Pe \gg R^{-2} \sigma^{-1}. \tag{7.2}$$

Therefore, (7.1) and (7.2) must both be satisfied to ensure the validity of the solution. The eigenfunction solution found upstream of any obstacle for $R = O(\epsilon^{\frac{1}{2}})$ will occur, however, if (7.1) is violated, but then the shear-layer structure is not that given in § 4. In that case, the linearity of the Ekman layer appends a restriction somewhat weaker than (7.1),

$$F \ll R.$$

Further study has shown that, if we abandon the non-diffusive restriction (7.2), a solution not unlike the one presented in §§ 3–6 may be found; the details there are a bit more complex, though the shear layers appear in that case to be Stewartson layers. Details will be given at a later time.

The author is grateful for the technical assistance of Messrs Adewale A. Adigun, Jack Fullerton and Scott Anderson in the course of this work. Thanks also to Odus R. Burggraf, Keith Stewartson, and one referee for helpful comments on an earlier numerical method for § 6.

This research was supported by the Atmospheric Research Section, National Science Foundation, under Grant nos. DES75–16084 and ATM77–07983.

Appendix

We seek solution to

$$\frac{\partial^3 v}{\partial \xi^3} = 4 \frac{\partial^2 v}{\partial z^2}, \tag{A 1}$$

in regions of semi-infinite or infinite extent in both ξ and z. Such solutions must be of self-similar type,

$$v = z^n F(\eta), \quad \eta \equiv \xi / (\tfrac{3}{4} z)^{\frac{4}{3}}. \tag{A 2}$$

Substitution of (A 2) into (A 1) yields

$$F''' - \eta^2 F'' + \tfrac{3}{2}(2n - \tfrac{5}{3}) \eta F' - \tfrac{9}{4} n(n-1) F = 0, \tag{A 3}$$

which may be solved by substituting into (A 3) the following:

$$F(\eta) = \int_a^b \exp(-ip\eta)\, Q(p)\, dp. \tag{A 4}$$

The ordinary differential equation that results for Q has 1/2-order Bessel function solutions which may be written as

$$Q = p^{-1-\frac{3n}{2}} \exp[\pm(1+i)(2^{\frac{1}{2}}/3)p^{\frac{3}{2}}]. \tag{A 5}$$

The end-points (a, b) of the integration path in the complex p plane must be such that

$$\left.\begin{aligned} p^2 Q \exp(-i\eta p)\big|_a^b &= 0, \\ [p^2 Q' + (3n - \tfrac{1}{2})\, pQ] \exp(-i\eta p)\big|_a^b &= 0. \end{aligned}\right\} \tag{A 6}$$

Since we are interested in solutions that are small, away from the corner region, we suppose that $n < 0$. In that case, a may be taken at the origin, from which point a branch cut extends along the negative real axis. Linearly independent solutions are H_n, $\bar{H}_n$, and G_n where

$$\left.\begin{aligned} H_n(\eta) &\equiv \int_0^\infty \frac{dp}{p^{1+3n/2}} \exp[-i\eta p - (1+i)(2^{\frac{1}{2}}/3)p^{\frac{3}{2}}], \\ G_n(\eta) &\equiv \int_0^\infty \frac{dr}{r^{1+3n/2}} \exp[r\eta - (2/3)r^{\frac{3}{2}}]. \end{aligned}\right\} \tag{A 7}$$

We notice that H_n is bounded for all η; G_n is bounded in $\eta < 0$ only.

Solution in $\frac{1}{4}$ plane: $\xi < 0, z > 0$

In the $\frac{1}{4}$ plane $\xi < 0, z > 0$, a solution to (A 1) is

$$v = z^n [A H_n(\eta) + \bar{A}\bar{H}_n(\eta) + B G_n(\eta)]. \tag{A 8}$$

The appropriate boundary conditions for eigenfunction solutions are

$$\left.\begin{aligned} v = \frac{\partial^2 v}{\partial \eta^2} = 0 \quad &\text{on} \quad \eta = 0, \quad z > 0, \\ v = 0 \qquad\quad &\text{on} \quad z = 0, \quad \eta < 0. \end{aligned}\right\} \tag{A 9}$$

We need the asymptotic forms of H_n and G_n for $\eta \to -\infty$ to apply the second of these conditions.

It is easy to show that

$$\left.\begin{aligned} H_n &\sim \exp[-i(3n\pi/4)]\,(-\eta)^{3n/2}\Gamma(-3n/2), \quad \eta \to -\infty, \\ G_n &\sim (-\eta)^{3n/2}\,\Gamma(-3n/2), \quad \eta \to -\infty. \end{aligned}\right\} \tag{A 10}$$

Thus

$$A \exp[-i(3n\pi/4)] + \bar{A} \exp[i(3n\pi/4)] + B = 0. \tag{A 11}$$

We also need special values of H_n and G_n at $\eta = 0$ to apply the other conditions in (A 9), namely

$$\left.\begin{aligned} H_n(0) &= (\tfrac{2}{3})^{1-n}\,\Gamma(-n)\exp(in\pi/4), \\ H_n''(0) &= (\tfrac{2}{3})^{-\frac{1}{3}-n}\,\Gamma(\tfrac{4}{3}-n)\exp[i(n\pi/4 - \tfrac{1}{3}\pi)], \\ G_n(0) &= (\tfrac{2}{3})^{1-n}\,\Gamma(-n), \\ G_n''(0) &= (\tfrac{2}{3})^{-\frac{1}{3}-n}\,\Gamma(\tfrac{4}{3}-n). \end{aligned}\right\} \tag{A 12}$$

Using (A 12) with (A 9) gives

$$\left.\begin{aligned} &A\exp(in\pi/4)+\bar{A}\exp(-in\pi/4)+B=0,\\ &A\exp[i(n\pi/4-\tfrac{1}{3}\pi)]+\bar{A}\exp[-i(n\pi/4-\tfrac{1}{3}\pi)]+B=0.\end{aligned}\right\} \tag{A 13}$$

Simultaneous solution of (A 10) and (A 13) leads to the characteristic equation

$$1-\cos n\pi-\frac{\sin(n\pi)}{3^{\frac{1}{2}}}=0,$$

which has solutions

$$n=-\tfrac{5}{3}+2l, \quad l=0,\ -1,\ -2,\ \ldots. \tag{A 14}$$

Solution in the $\frac{3}{4}$ plane: $\xi<0, z<0; z>0$

In a similar fashion one can construct a solution to (A 1) in $\xi<0, z<0, z>0$:

$$v=z^n[AH_n(\eta)+\bar{A}\bar{H}_n(\eta)], \quad z>0,$$

$$v=(-z)^n[BH_n(\eta)+\bar{B}\bar{H}_n(\eta)+CG_n(\eta)], \quad z<0, \quad \xi<0.$$

The homogenous conditions to be used are

$$v=\frac{\partial^2 v}{\partial\eta^2}=0 \quad \text{on} \quad \eta=0, \quad z<0,$$

$$v=0 \qquad\quad \text{on} \quad z=0, \quad \xi>0,$$

and the solutions must be appropriately joined on $z=0$, by requiring continuity of v and $\partial v/\partial z$. Those five conditions serve to determine A, B, and C in the same way as before. The characteristic equation in this case is

$$\sin(3n\pi/2)\cos(n\pi-\tfrac{1}{6}\pi)=0.$$

There is obviously a double infinity of values of n satisfying this equation, namely

$$\left.\begin{aligned} &n=\tfrac{2}{3}k, \quad k=-1,\ -2,\ \ldots,\\ &n=\tfrac{2}{3}+l, \quad l=-1,\ -2,\ \ldots.\end{aligned}\right\} \tag{A 15}$$

The largest few values are $-\frac{1}{3}$, $-\frac{2}{3}$, $-\frac{4}{3}$, -2, $-\frac{7}{3}$, ...

Significance of the solutions

In connexion with the solutions to the shear layer discussed in §5, we raised the question of possible singularities of the solution, connected with Ekman-layer eruption at $\xi=0$, $z=0$ and at $\xi=0$, $z=d$. Considering the $\frac{1}{4}$-plane solution first, with $w=-2\partial v/\partial z$, (A 8) and considerable algebra leads to

$$\int_{-\infty}^{0} w\,d\xi=2\times 3^{\frac{1}{2}}z^{n-\frac{1}{3}}(\tfrac{3}{2})^n\,\Gamma(\tfrac{1}{3}-n)\,B, \tag{A 16}$$

so we see that no $n<0$ leads to a finite source at the corner in the $\frac{1}{4}$ plane. Similar analysis of the $\frac{3}{4}$-plane solutions leads to

$$\int_{0}^{\infty} w\,d\xi=2\times 3^{\frac{1}{2}}z^{n-\frac{1}{3}}(\tfrac{3}{2})^n\,\Gamma(\tfrac{1}{3}-n)\,\mathrm{Re}\,(A\exp[i(\tfrac{1}{4}n\pi-\tfrac{1}{3}\pi)]). \tag{A 17}$$

Again, no value of $n < 0$ leaves (A 17) bounded for $z \to 0$. Then, we conclude, no source-like singularities exist, for $n < 0$.

If we look for solutions with doublet-like structure, we find, for the $\frac{1}{4}$ plane, that

$$m_d \equiv \int_{-\infty}^{0} \xi w \, d\xi = -\tfrac{9}{2}\, 3^{\frac{1}{3}} (\tfrac{3}{2})^n z^{n+\frac{1}{3}} \Gamma(-n-\tfrac{1}{3}) \operatorname{Im}(A \exp[in\pi/4]). \tag{A 18}$$

Since $n = -\frac{1}{3}$ is *not* an eigenvalue in the $\frac{1}{4}$-plane problem [see (A 14)], there is no $\frac{1}{4}$-plane singularity with a finite value of m_d as $z \to 0$. However, $n = -\frac{1}{3}$ *is* an eigenvalue for the $\frac{3}{4}$-plane problem [see (A 15)], so that

$$m_d = -\tfrac{1}{2} \times 3^{\frac{4}{3}} z^{n+\frac{1}{3}} \Gamma(-n-\tfrac{1}{3}) \, Re(A \exp[i(\tfrac{1}{4}n\pi + \tfrac{1}{3}\pi)]), \tag{A 19}$$

shows a finite value for $z \to 0$ in that case.

In summary, the $\frac{1}{4}$-plane solution has no source or doublet singularities; the $\frac{3}{4}$ plane *does* possess a doublet singularity for $n = -\frac{1}{3}$. It should be noted that other eigenvalues in the lists (A 14) and (A 15) correspond to finite values of other higher integral moments of w. Those singularities are equivalent to, so far as the overall shear layer solution of § 5 is concerned, more and more singular generalized functions like $\delta''(z-d)$, etc.

REFERENCES

Barnard, B. J. S. & Pritchard, W. G. 1975 *J. Fluid Mech.* **71**, 43.

Foster, M. R. 1977 *Z. angew. Math. Phys.* **28**, 55.

Graebel, W. P. 1969 *Quart. J. Mech. Appl. Math.* **22**, 39.

Greenspan, H. P. 1969 *The Theory of Rotating Fluids*. Cambridge University Press.

Janowitz, G. S. 1971 *J. Fluid Mech.* **47**, 171.

Martin, S. & Long, R. R. 1968 *J. Fluid Mech.* **31**, 669.

Moore, D. W. & Saffman, P. G. 1969 *Phil. Trans. Roy. Soc.* A **264**, 597.

Stewartson, K. 1964 *The Theory of Laminar Boundary Layers in Compressible Fluids*. Oxford University Press.

Yih, C. S. 1969 *Ann. Rev. Fluid Mech.* **1**, 73.